Magic Nature of Neutrons in ^{54}Ca: First Mass Measurements of ^{55–57}Ca

S. Michimasa *et al.*

Phys. Rev. Lett. **121**, 022506 — Published 11 July 2018

DOI: 10.1103/PhysRevLett.121.022506

Magic nature of neutrons in ^{54}Ca: First mass measurements of $^{55-57}$Ca

S. Michimasa,[1,*] M. Kobayashi,[1] Y. Kiyokawa,[1] S. Ota,[1] D. S. Ahn,[2] H. Baba,[2] G. P. A. Berg,[3] M. Dozono,[1] N. Fukuda,[2] T. Furuno,[4] E. Ideguchi,[5] N. Inabe,[2] T. Kawabata,[4] S. Kawase,[6] K. Kisamori,[1] K. Kobayashi,[7] T. Kubo,[8,9] Y. Kubota,[2] C. S. Lee,[1] M. Matsushita,[1] H. Miya,[1] A. Mizukami,[10] H. Nagakura,[7] D. Nishimura,[11] H. Oikawa,[10] H. Sakai,[2] Y. Shimizu,[2] A. Stolz,[9] H. Suzuki,[2] M. Takaki,[1] H. Takeda,[2] S. Takeuchi,[12] H. Tokieda,[1] T. Uesaka,[2] K. Yako,[1] Y. Yamaguchi,[1] Y. Yanagisawa,[2] R. Yokoyama,[13] K. Yoshida,[2] and S. Shimoura[1]

[1] *Center for Nuclear Study, The University of Tokyo, 2-1 Hirosawa, Wako, Saitama 351-0198, Japan*
[2] *RIKEN Nishina Center for Accelerator-Based Science, 2-1 Hirosawa, Wako, Saitama 351-0198, Japan*
[3] *Department of Physics and Joint Institute for Nuclear Astrophysics, University of Notre Dame, Notre Dame, Indiana 46556, USA*
[4] *Department of Physics, Kyoto University, Kitashirakawa-Oiwake, Sakyo, Kyoto 606-8502, Japan*
[5] *Research Center for Nuclear Physics, Osaka University, 10-1 Mihogaoka, Ibaraki, Osaka 567-0047, Japan*
[6] *Department of Advanced Energy Engineering Sciences, Kyushu University, 6-1 Kasuga-koen, Kasuga, Fukuoka 816-8580, Japan*
[7] *Department of Physics, Rikkyo University, Toshima, Tokyo 171-8501, Japan*
[8] *Facility for Rare Isotope Beams, Michigan State University, 640 S Shaw Lane, East Lansing, Michigan 48824, USA*
[9] *National Superconducting Cyclotron Laboratory, Michigan State University, 640 S Shaw Lane, East Lansing, Michigan 48824, USA*
[10] *Department of Physics, Tokyo University of Science, Noda, Chiba 278-8510, Japan*
[11] *Department of Physics, Tokyo City University, Tamazutsumi 1-28-1, Setagaya-ku, Tokyo 158-8557, Japan*
[12] *Department of Physics, Tokyo Institute of Technology, Meguro, Tokyo 152-8551, Japan*
[13] *Department of Physics and Astronomy, the University of Tennessee, Knoxville, Tennessee 37996, USA*

(Dated: April 23, 2018)

We have performed the first direct mass measurements of neutron-rich calcium isotopes beyond neutron number 34 at the RIKEN Radioactive Isotope Beam Factory by using the time-of-flight magnetic-rigidity technique. The atomic mass excesses of $^{55-57}$Ca were determined for the first time to be $-18650(160)$ keV, $-13510(250)$ keV, and $-7370(990)$ keV, respectively. We examined the emergence of neutron magicity at $N = 34$ based on the new atomic masses. The new masses provided experimental evidence for the appearance of a sizable energy gap between neutron $2p_{1/2}$ and $1f_{5/2}$ orbitals in ^{54}Ca, comparable to the gap between neutron $2p_{3/2}$ and $2p_{1/2}$ orbitals in ^{52}Ca. For the ^{56}Ca nucleus, an open-shell property in neutrons is suggested.

PACS numbers: 21.10.Dr, 27.40.+z, 29.38.Db

The atomic nucleus has shell structures for both protons and neutrons with significant energy gaps occurring at particular occupation numbers. These numbers are called 'magic numbers' in analogy to the shell structure of noble gases in atomic physics. The magic numbers, $N, Z = 2$, 8, 20, 28, 50, 82, and 126, suggested by Mayer and Jensen [1, 2] are well established in nuclei on or near the valley of stability.

When advanced high-intensity radioactive isotope (RI) beam facilities became available, it became possible to explore properties of exotic nuclei far from the β-stability line towards the boundary of existence, called the proton and neutron drip lines. Measurements away from the valley of stability revealed that the magic numbers are not invariant in the entire nuclear chart. The properties of closed shells at $N = 8$, 20, and 28 are less distinct in the neutron-rich mass region [3–10]. On the other hand, it was reported that a new magic number emerges at $N = 16$ near the neutron drip line of oxygen isotopes [11]. Also at $N = 32$, the occurrence of significant subshell energy gap was experimentally demonstrated in the nuclear region from Ar to Cr nuclei [12–18].

In response to these experimental data, many theoretical studies were intensively carried out to understand these structural changes in nuclei far from β stability and to qualitatively predict the behavior of the nuclear structure near the drip line. As an important milestone, the emergence of a subshell closure at $N = 34$ remains a controversial topic. The theoretical prediction based on the strongly attractive interaction between $1f_{7/2}$ protons and $1f_{5/2}$ neutrons [19] indicates a similar migration of neutron $2p_{3/2}$, $2p_{1/2}$ and $1f_{5/2}$ single-particle levels at $N = 34$ as observed at $N = 29$ [20]. Later, Steppenbeck *et al.* observed a high 2_1^+ excitation energy at 2043(19) keV in ^{54}Ca suggesting that the neutrons in ^{54}Ca undergo sizable subshell closure [21]. However, discrepancies on the emergence of the $N = 34$ subshell closure in neutron-rich Ca region remain even among the theories predicting the 2_1^+ energy of approximately 2.0 MeV [22–24].

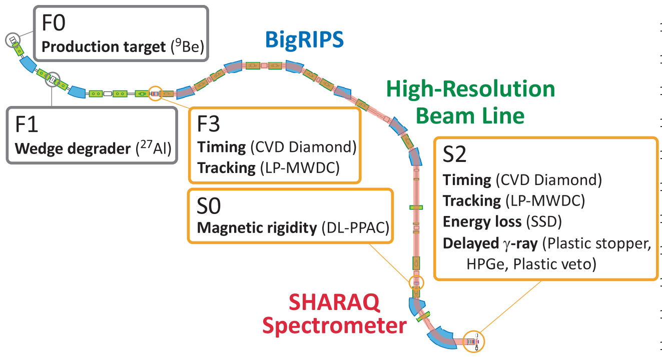

FIG. 1. Schematic layout of the detectors installed in the BigRIPS separator, the High-Resolution Beam Line, and the SHARAQ spectrometer.

In this Letter, we present the first mass measurements of the exotic calcium isotopes $^{55-57}$Ca, and determine the neutron single-particle structure in neutron-rich calcium isotopes by using "filtering functions" of the atomic masses, that will be defined below, for estimating gap energies in the single-particle spectra.

The present experimental study was performed at the Radioactive Isotope Beam Factory (RIBF) at RIKEN, which is operated by RIKEN Nishina Center and Center for Nuclear Study, University of Tokyo. The masses were measured directly by the time-of-flight magnetic-rigidity (TOF-$B\rho$) method [25, 26] with a flight path of approximately 100 m from the BigRIPS separator [27] to the SHARAQ spectrometer [28].

Neutron-rich isotopes were produced by fragmentation of a ^{70}Zn primary beam at 345 MeV/u in a ^{9}Be target with a thickness of 2.2 g/cm^2. The fragments were separated by BigRIPS and transported in the High-Resolution Beam Line (HRB) to the SHARAQ spectrometer. A wedge degrader of 0.27 g/cm^2 was used at the BigRIPS focus F1 to remove the high flux of lower-Z fragments.

The beam line and SHARAQ were operated in the dispersion matching mode which a momentum resolution of better than 15000 [29] at the focal plane with an intermediate dispersion. A schematic layout of the beam line with the locations of the detectors used in the experiment is shown in Fig. 1. The time of flight (TOF) was measured with newly developed CVD diamond detectors [30] installed at F3 and S2. The flight path length between F3 and S2 was 105 m along the central ray. The typical TOF was 540 ns. Because of the relatively low count rate of fragments at approximately 2000 particles per second, it is assured that all measurements belonged to a single particle. A slit at F1 was set to restrict the momentum spread of fragments to ±0.5 %. This setting was adopted to obtain broadly distributed fragments within the momentum acceptance against the energy-loss difference in the detectors depending on their atomic numbers. We installed two low-pressure multi-wire drift chambers (LP-MWDCs) [31] at both focal planes F3 and S2 to correct for the flight path differences within the acceptance on an event-by-event basis. The magnetic rigidity was determined using a delay-line parallel-plate avalanche counter (DL-PPAC) [32] located at S0. To determine the atomic number of the fragments, we used two silicon strip detectors (SSDs) at the focal plane S2. A detector system consisting of a plastic stopper, two HPGe clover detectors [33] and a plastic veto detector was installed downstream of S2 to estimate the flux of isomeric states in the fragmented nuclei [34].

The mass of a fragment m is determined by the simultaneous measurement of charge q, TOF t, magnetic rigidity $B\rho$ and flight path length L between the timing detectors by using the equation:

$$\frac{m}{q} = \frac{B\rho}{\gamma L}t = \frac{B\rho}{c}\sqrt{\left(\frac{ct}{L}\right)^2 - 1}, \tag{1}$$

where γ is the Lorentz factor. To determine nuclear masses accurately, it is crucial to determine accurately the ion-optical parameters for L and $B\rho$ from the tracking data. Since we measured $B\rho$ of the fragments at S0 that was located in the middle of the flight path, TOF and beam trajectory of the fragments were affected by energy loss and multiple scattering in the DL-PPAC at S0. To take into account such effects, the $B\rho$ differences of the fragments relative to the central ray between F3 and S0 (S0 and S2) were tagged by the horizontal hit position at S0 relative to that at F3 (S2). Furthermore, the path length from F3 to S0 (S0 to S2) was also calculated precisely from the momentum vector of the beam at F3 (S2) and the $B\rho$ difference in the corresponding part. In accordance with the Taylor expansion of Eq. (1) with the hit positions and angles at both F3 and S2 and the horizontal hit position at S0 in addition to the TOF between F3 and S2, we considered the mass-to-charge ratio (m/q) as a fourth-order polynomial function of these observed parameters. Since this procedure took into account the transport matrix elements of the beam line up to fourth order, the atomic masses could be determined with a sufficient degree of accuracy. The coefficients of respective terms of this Taylor-expanded function were determined by a multiple polynomial regression of the ion-optical data of reference masses which was simultaneously measured in the same setting. The reference nuclei were $^{52-54}$Ca ,$^{49,51-53}$K, $^{46-48}$Ar, $^{43-46}$Cl, ^{41,42}S, $^{38-42}$P, and $^{36-40}$Si [16, 17, 35, 36], where the atomic masses were determined with precisions of better than 320 keV. Also as reference masses, only nuclei were selected where long-lived isomeric excited states ($T_{1/2}$ > 100 ns) were not reported so far and were not identified by the HPGe detectors used in the present experiment, because the isomeric states cause an ambiguity in the mass calibration by their excitation energies.

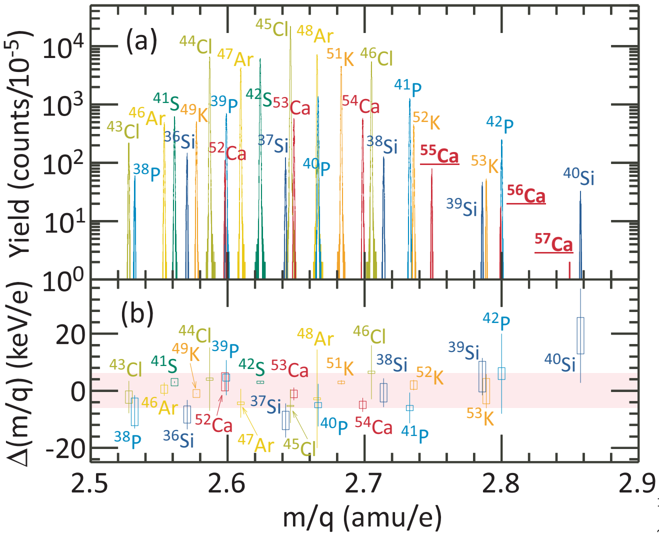

FIG. 2. (a) Measured m/q spectrum of reference masses and Ca isotopes. The underlined isotopes indicate the masses newly determined in the present experiment. (b) m/q difference between the present and the AME2016 database [38]. The boxes (bars) show statistical errors of the present measurement (the total errors in the AME2016). The red-colored band displays the systematic error of calibration accuracy in the present measurement.

The m/q values calibrated by the above procedure showed small shifts depending on the atomic numbers. The previous works using the TOF-$B\rho$ method [36, 37] reported the need to correct a Z dependence in the mass calibration procedure. In the present experiment, this is because the m/q spectra obtained by higher-order ion-optical corrections involve higher-order moments of a distribution, such as skewness, linked in error distributions of the tracking detectors. Based on a Z dependence in the detectors' resolutions and higher-order aberrations of the beam line, a correlation between the shift and the atomic number of fragments was considered to be mainly quadratic. Since a reasonable correlation was phenomenologically identified in the present data, the peak shifts were corrected by using a quadratic function of Z. The correction functions for the ion optics and the Z dependence were fixed after iterative examinations using the reference masses.

Figure 2(a) shows the measured m/q spectrum of the reference masses and Ca isotopes, where the masses of underlined nuclei are newly determined in the present experiment. A root-mean-square resolution of 9.85×10^{-5} was achieved for ^{55}Ca. Figure 2(b) shows the m/q differences of the present measurement and the reported values in the AME2016 database [38]. The boxes and bars show statistical errors estimated in the present measurement and the errors of masses reported in the AME2016, respectively. The m/q values of the reported isotopes were systematically reproduced within an error of 6.1 keV/e, which is perceived as the systematic errors [25] in this measurement. The systematic error of the Z-dependence correction was estimated to be 3.3 keV/e for Ca isotopes from the errors of the deduced correction function. The total errors of measured masses were attributed to those two systematic errors in addition to the statistical error.

TABLE I. The atomic mass excesses determined in the present experiment and the AME2016 database [38].

Nucleus	Present (keV)	AME2016 (keV)
^{57}Ca	−7370(990)	—
^{56}Ca	−13650(250)	—
^{55}Ca	−18650(160)	—
^{48}Ar	−22330(120)	−22280(310)
^{46}Cl	−13700(110)	−13860(210)
^{44}Cl	−20540(110)	−20380(140)
^{42}P	+1100(100)	+1010(310)
^{40}P	−8150(100)	−8110(150)
^{40}Si	+5700(130)	+5430(350)

The neutron-rich calcium isotopes yielded 3379 events for ^{55}Ca, 619 events for ^{56}Ca, and 29 events for ^{57}Ca, respectively. The atomic mass excesses of $^{55-57}$Ca were determined to be −18650(160) keV, −13650(250) keV and −7370(990) keV, respectively, as summarized in Table. I. The table also shows the reference mass excesses with accuracies improved by the present measurement. The resulting values were −22330(120) keV in ^{48}Ar, −13700(110) keV in ^{46}Cl, −20540(110) keV in ^{44}Cl, +1100(100) keV in ^{42}P, −8150(100) keV in ^{40}P, and +5700(130) keV in ^{40}Si.

The two-neutron separation energies (S_{2n}) of calcium isotopes are shown in Fig. 3(a). The newly determined S_{2n} values are shown as red squares with error bars. The solid (open) circles with errors display literature (evaluation) values from the AME2016. The lines show the following theoretical predictions. MBPT [39] (solid pale-rose) and IM-SRG [40] (solid green) represent advanced microscopic calculations including three-nucleon forces. KB3G [41] (dashed aqua) and modified SDPF-MU [42] (dashed red) show the results of shell model calculations by using the corresponding two-body interactions with phenomenological corrections. FRDM12 [43] (dotted burgundy), HFB24 [44] (dotted yellow) and KUTY05 [45] (dotted gray) are often-cited, global nuclear mass predictions.

Figure 3(b) shows the differences between theoretical and experimental S_{2n} values. The AME2016 evaluations for $^{55-57}$Ca are consistent with the present results within 1σ errors. The theoretical predictions shown are distributed over several MeV. The calculations with the MBPT and KB3G interactions reproduce the present results well. The calculations by modified SDPF-MU and IM-SRG predict that $^{55-57}$Ca are loosely-bound though they provide good agreements for $^{48-54}$Ca. The

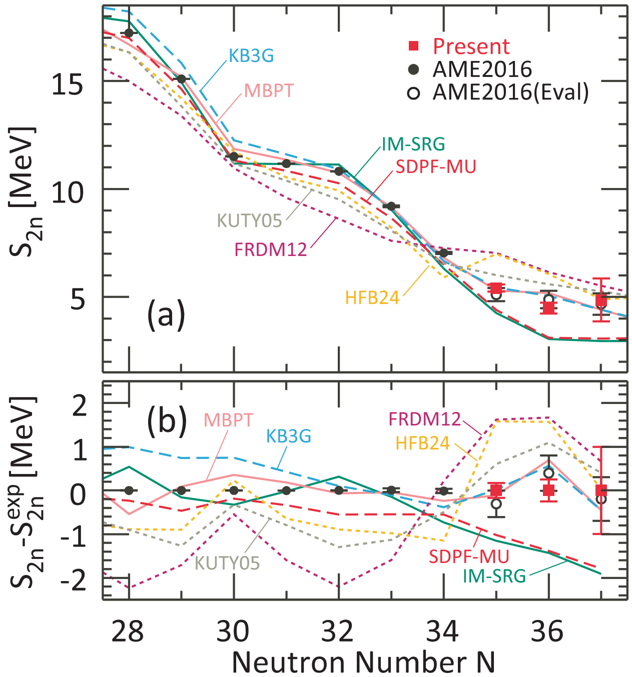

FIG. 3. (a) The two-neutron separation energies ($S_{2\mathrm{n}}$) of Ca isotopes as a function of the neutron number. (b) The differences of theoretical $S_{2\mathrm{n}}$ from the experimental values. The symbols and lines are common in both figures: The red squares show the present results. The solid (open) circles are literature values from the AME2016 database (evaluation). The colored lines show theoretical predictions. For notations see text.

FRDM12, HFB24, and KUTY05 show a similar trend. They predict smaller values around $N = 28$ and 32 and larger values at $N = 34$ and 35.

We now discuss the magic nature at $N = 34$ in Ca isotopes based on the measured atomic masses. In a simple picture, the magic number is illustrated by an occupation number of a nucleon, at which energetically lower single-particle orbitals are completely filled and an additional nucleon settles in an upper orbital with a large energy gap. This picture of magic number is known to be too simple in the theoretical point of view since real nucleons contained in a nucleus strongly interact with each other. Empirical indexes for evaluating the energy gap of the single-particle spectrum in nuclei [46, 47] have been suggested based on experimental systematics and theoretical understanding. We describe the magic nature of Ca isotopes by using the empirical mass filters.

W. Satuła *et al.* [46] suggested to express the energy gaps of single-particle spectra empirically by the following filtering function (δe) using the atomic masses of neighboring nuclei:

$$\delta e = 2\left[\Delta_3(N) - \Delta_3(N-1)\right] = S_{2\mathrm{n}}(N) - S_{2\mathrm{n}}(N+1), \tag{2}$$

in cases of even N. $\Delta_3(N)$ is the three-point mass difference in a nucleus with a fixed number of protons and N neutrons and explicitly represented by

$$\Delta_3(N) = \frac{(-1)^N}{2}\left[M(N+1) - 2M(N) + M(N-1)\right], \tag{3}$$

where $M(N)$ shows the atomic mass of the nucleus with N neutrons. This quantity is known as the odd-even mass parameter of second difference [20]. It is remarkable that the Δ_3 at odd N can be associated with the pairing gap [48].

We note here the difference between δe and the empirical two-neutron shell gap $\Delta_{2\mathrm{n}} \equiv S_{2\mathrm{n}}(N) - S_{2\mathrm{n}}(N+2)$ [47] that is frequently used to demonstrate a shell-gap evolution in nuclei. The $\Delta_{2\mathrm{n}}$ shell gap closely links to the δe through the relation:

$$\Delta_{2\mathrm{n}} = 2\left[\delta e - \Delta_3(N+1) + \Delta_3(N-1)\right], \tag{4}$$

where N is an even number. Hence, the $\Delta_{2\mathrm{n}}$ shell gap is affected by the difference of pairing gaps in the highest-occupied and lowest-open orbitals in addition to δe. Since the pairing gaps in the $\nu(2p_{3/2})$ and $\nu(2p_{1/2})$ orbitals are known to be different in the Ca isotopes [49], the δe is considered to be better suited for the discussion on the single-particle gap in ^{54}Ca than the $\Delta_{2\mathrm{n}}$ shell gap.

The systematic trend of the δe shell gap for neutron-rich Ca isotopes is shown in Fig. 4(a) and compared to the same theoretical predictions as shown in Fig. 3. The δe value of ^{54}Ca is comparable to that of ^{52}Ca and slightly smaller than that of ^{48}Ca. This denotes that ^{54}Ca has a magic nature of neutrons as is the case of ^{52}Ca. The δe value of ^{56}Ca is smaller than those of ^{48,52,54}Ca, having the neutron magicity, and thus it is suggested that in ^{56}Ca occupied and unoccupied neutron orbitals are packed near the Fermi surface. The theories cannot completely reproduce the evolution of δe of Ca isotopes as a function of the neutron numbers. The KB3G calculations show a reduction from $N = 32$ to 34. The MBPT calculations reproduce well the energy gaps in ^{52,54}Ca, however the δe of ^{48}Ca is smaller than those of ^{52,54}Ca. The IM-SRG prediction reproduce the data with relatively good accuracy in this region, but its variation is slightly larger than the experiment.

Figure 4(b) shows the δe shell gaps for $N = 34$ (square) and 36 (diamond) as a function of the atomic number in comparison with $N = 32$ (circle). The present values are shown as red symbols. The other values were obtained from the AME2016 database and the newly-reported masses in $^{52-55}$Ti isotopes [50]. Along the $N = 32$ and 34 chains, the δe values in Ca increase approximately 1.5 times compared to the constant values around $Z = 25$ (Mn). However, the small δe in ^{55}Sc and the large δe in ^{53}Sc suggest that in Sc isotopes the $N = 32$ energy gap emerges but there is no gap at $N = 34$. Therefore, it is suggested that the energy difference between the $\nu(2p_{1/2})$ and $\nu(1f_{5/2})$ orbitals becomes large from Sc to Ca. Meanwhile, the δe values at $N = 36$ are small across

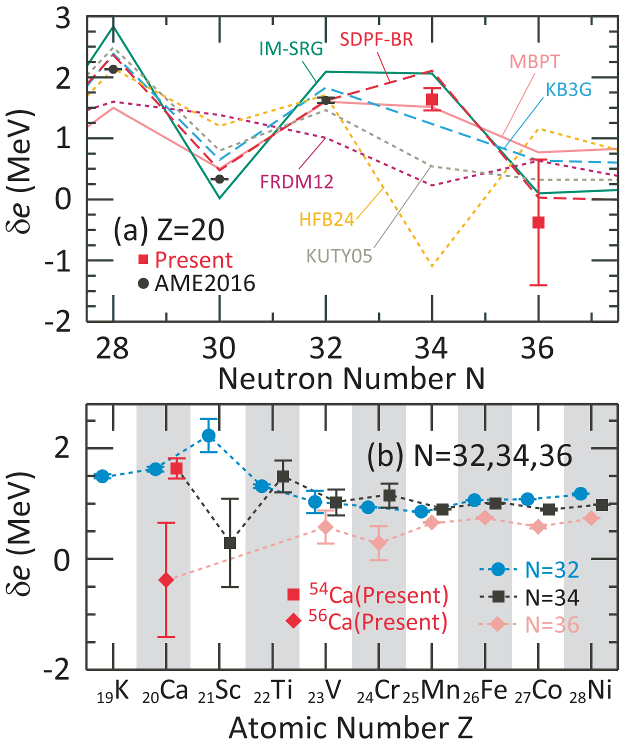

FIG. 4. Systematics of the empirical energy gaps (δe) of single-particle spectra. (a) Ca isotopes are shown with theoretical predictions. The present results are shown as red squares and the solid circles are literature values from the AME2016 database. The theoretical predictions are shown by lines with the same colors as described in Fig. 3. (b) Isotonic chains at $N = 32$, 34, and 36 as a function of atomic number are shown. The circles, squares and diamonds refer to $N = 32$, 34 and 36, respectively. The present results are shown as red symbols. The other values were obtained from the AME2016 and Ref. [50].

$Z = 20 - 28$, and comparable with the δe of the $N = 30$ isotope, ^{50}Ca (*see* Fig. 4(a)). Therefore, it is suggested that ^{56}Ca has an open-shell character for neutrons similar to other $N = 36$ isotones. This is reasonably interpreted by a picture that the valence neutrons partly fill the $1f_{5/2}$ orbital beyond the $N = 34$ gap.

In conclusion, the atomic masses of the neutron-rich calcium isotopes $^{55-57}$Ca were measured by using the TOF-$B\rho$ method and determined for the first time. By observation of the mass evolution in Ca isotopes beyond $N = 34$, the magic nature at $N = 34$ in the neutron-rich Ca region became evident. The energy gap of the single-neutron spectrum in ^{54}Ca was evaluated to be comparable with that in ^{52}Ca based on the experimental δe shell gaps. Also, it was experimentally shown that the energy gaps of single-neutron spectra in the $N = 34$ isotones become significant from Sc to Ca. The δe shell gap in ^{56}Ca suggests an open-shell character for neutrons. The δe values in ^{54,56}Ca indicate that the closure of the $\nu(2p_{1/2})$ orbital causes the magicity at $N = 34$.

We thank the RIKEN Nishina Center and the Center for Nuclear Study, the University of Tokyo accelerator staff for the excellent beam delivery. We also thank Prof. N. Shimizu for fruitful discussions. This work is financially supported in part by JSPS KAKENHI Grant No. JP22740150. M.K is grateful to the JSPS for a Research Fellowship for young scientists under program No. JP14J03376. G.B. acknowledges support by the National Science Foundation through Grant No. PHY-1068192 and The Joint Institute for Nuclear Astrophysics Center for the Evolution of the Elements through Grants No. PHY-0822648 and No. PHY-1430152.

* mitimasa@cns.s.u-tokyo.ac.jp

[1] M. G. Mayer, Phys. Rev. **75**, 1969 (1949).
[2] O. Haxel, J. H. D. Jensen, and H. E. Suess, Phys. Rev. **75** 1766 (1949).
[3] A. Navin *et al.*, Phys. Rev. Lett. **85**, 266 (2000).
[4] H. Iwasaki *et al.*, Phys. Lett. B **481**, 7 (2000).
[5] H. Iwasaki *et al.*, Phys. Lett. B **491**, 8 (2000).
[6] S. Shimoura *et al.*, Phys. Lett. B **560**, 31 (2003).
[7] C. Thibault, R. Klapisch, C. Rigaud, A. M. Poskanzer, R. Prieels, L. Lessard, and W. Reisdorf, Phys. Rev. C **12** 644 (1975).
[8] T. Motobayashi *et al.*, Phys. Lett. B **346**, 9 (1995).
[9] B. Bastin *et al.*, Phys. Rev. Lett. **99**, 022503 (2007).
[10] S. Takeuchi *et al.*, Phys. Rev. Lett. **109**, 182501 (2012).
[11] A. Ozawa, T. Kobayashi, T. Suzuki, K. Yoshida, and I. Tanihata, Phys. Rev. Lett. **84**, 5493 (2000).
[12] J. I. Prisciandaro *et al.*, Phys. Lett. B **510**, 17 (2001).
[13] R. V. F. Janssens *et al.*, Phys. Lett. B **546**, 55 (2002).
[14] A. Huck, G. Klotz, A. Knipper, C. Miehé, C. Richard-Serre, G. Walter, A. Poves, H. L. Ravn, and G. Marguier, Phys. Rev. C **31**, 2226 (1985).
[15] A. Gade *et al.*, Phys. Rev. C **74**, 021302(R) (2006).
[16] F. Wienholtz *et al.*, Nature **498**, 346 (2013).
[17] M. Rosenbusch *et al.*, Phys. Rev. Lett. **114**, 202501 (2015).
[18] D. Steppenbeck *et al.*, Phys. Rev. Lett. **114**, 252501 (2015).
[19] T. Otsuka, R. Fujimoto, Y. Utsuno, B. A. Brown, M. Honma, and T. Mizusaki, Phys. Rev. Lett. **87**, 082502 (2001).
[20] A. Bohr and B. R. Mottelson, *Nuclear Structure* (World Scientific, Singapore,1988), Vol. I.
[21] D. Steppenbeck *et al.*, Nature **502**, 207 (2013).
[22] L. Coraggio, A. Covello, A. Gargano, and N. Itaco, Phys. Rev. C **80**, 044311 (2009).
[23] T. Otsuka, T. Suzuki, J. D. Holt, A. Schwenk, and Y. Akaishi, Phys. Rev. Lett. **105**, 14 (2010).
[24] G. Hagen, M. Hjorth-Jensen, G. R. Jansen, R. Machleidt, and T. Papenbrock, Phys. Rev. Lett. **109**, 032502 (2012).
[25] A. Gillibert *et al.*, Phys. Lett. B **176**, 317 (1986).
[26] D. J. Vieira, J. M. Wouters, K. Vaziri, R. H. Kraus, H. Wollnik, G. W. Butler, F. K. Wohn, and A. H. Wapstra, Phys. Rev. Lett. **57**, 3235 (1986).
[27] T. Kubo, Nucl. Instrum. Methods Phys. Res., Sect. B **204**, 97 (2003).
[28] T. Uesaka, S. Shimoura, and H. Sakai, Prog. Theor. Exp.

Phys. **2012**, 03C007 (2012).

[29] S. Michimasa *et al.*, Nucl. Instrum. Methods Phys. Res., Sect. B **317**, 305 (2013).

[30] S. Michimasa *et al.*, Nucl. Instrum. Methods Phys. Res., Sect. B **317**, 710 (2013).

[31] H. Miya *et al.*, Nucl. Instrum. Methods Phys. Res., Sect. B **317**, 701 (2013).

[32] H. Kumagai, A. Ozawa, N. Fukuda, K. Sümmerer, and I. Tanihata, Nucl. Instrum. Methods Phys. Res., Sect. A **470**, 562 (2001).

[33] K. Hosomi *et al.*, Prog. Theor. Exp. Phys. **2015**, 081D01 (2015).

[34] S. Michimasa *et al.*, PoS(INPC2016) **106**, 1 (2017).

[35] M. Wang, G. Audi, A. H. Wapstra, F. G. Kondev, M. MacCormick, X. Xu, and B. Pfeiffer, Chinese Phys. C **36**, 1603 (2012).

[36] Z. Meisel *et al.*, Phys. Rev. Lett. **114**, 022501 (2015).

[37] M. Matoš *et al.*, Nucl. Instrum. Methods Res. Sect. A **696**, 171 (2012).

[38] Meng Wang, G. Audi, F. G. Kondev, W. J. Huang, S. Naimi, and Xing Xu, Chinese Phys. C **41**, 030003 (2017).

[39] J. D. Holt, T. Otsuka, A. Schwenk, and T. Suzuki, J. Phys. G: Nucl. Part. Phys. **39**, 085111 (2012).

[40] S. R. Stroberg, A. Calci, H. Hergert, J. D. Holt, S. K. Bogner, R. Roth, and A. Schwenk, Phys. Rev. Lett. **118**, 032502 (2017).

[41] A. Poves, J. Sánchez-solano, E. Caurier, and F. Nowacki, Nucl. Phys. A **694**, 157 (2001).

[42] Y. Utsuno, T. Otsuka, B. A. Brown, M. Honma, T. Mizusaki, and N. Shimizu, Phys. Rev. C **86**, 051301 (2012).

[43] P. Möller, A. J. Sierk, T. Ichikawa, and H. Sagawa, At. Data Nucl. Data Tables **109**–**110**, 1 (2016).

[44] S. Goriely, N. Chamel, and J. M. Pearson, Phys. Rev. C **88**, 024308 (2013).

[45] H. Koura, T. Tachibana, M. Uno, and M. Yamada, Prog. Theor. Phys. **113**, 305 (2005).

[46] W. Satuła, J. Dobaczewski, and W. Nazarewicz, Phys. Rev. Lett. **81**, 3599 (1998).

[47] D. Lunney, J. M. Pearson, and C. Thibault, Rev. Mod. Phys. **75**, 1021 (2003).

[48] S. A. Changizi, Chong Qi and R. Wyss, Nucl. Phys. A **940**, 210 (2015).

[49] B. A. Brown, Phys. Rev. Lett. **111**, 162502 (2013).

[50] E. Leistenschneider *et al.*, Phys. Rev. Lett. **120**, 062503 (2018).